

# 1 ‘One Health’ Genomic Surveillance of Avian and Human 2 Influenza A Viruses Through Environmental Wastewater 3 Monitoring

4

5 Andrew J. Lee <sup>1</sup>, Stephen Carson <sup>1</sup>, Marina I. Reyne <sup>1</sup>, Andrew Marshall <sup>1</sup>, Daniel Moody <sup>1</sup>,  
6 Danielle M. Allen <sup>1</sup>, Pearce Allingham <sup>1</sup>, Ashley Levickas <sup>1</sup>, Arthur Fitzgerald <sup>3</sup>, Stephen H.  
7 Bell <sup>1</sup>, Jonathan Lock <sup>1</sup>, Jonathon D. Coey <sup>1</sup>, Cormac McSparron <sup>2</sup>, Behnam F. Nejad <sup>2</sup>,  
8 David G. Courtney <sup>3</sup>, Gisli G. Einarsson <sup>4</sup>, James P. McKenna <sup>5</sup>, Derek J. Fairley <sup>5</sup>, Tanya  
9 Curran <sup>5</sup>, Jennifer M. McKinley <sup>2</sup>, Deirdre F. Gilpin <sup>4</sup>, Ken Lemon <sup>6</sup>, John W. McGrath <sup>1,7</sup>  
10 and Connor G. G. Bamford <sup>1,7</sup>.

11

## 12 **Author affiliations:**

13 <sup>1</sup> School of Biological Sciences, Queen’s University Belfast, 19 Chlorine Gardens, Belfast,  
14 BT9 5DL, Northern Ireland (UK).

15 <sup>2</sup> Geography, School of Natural and Built Environment, Queen’s University Belfast, Elmwood  
16 Avenue, Belfast, BT9 6AZ, Northern Ireland (UK).

17 <sup>3</sup> Wellcome-Wolfson Institute for Experimental Medicine, School of Medicine, Dentistry and  
18 Biomedical Sciences, Queen’s University Belfast, 97 Lisburn Road, Belfast, BT9 7BL,  
19 Northern Ireland (UK).

20 <sup>4</sup> School of Pharmacy, Queen’s University Belfast, 97 Lisburn Road, Belfast, BT9 7BL,  
21 Northern Ireland (UK).

22 <sup>5</sup> Regional Virology Laboratory (RVL), Belfast Health and Social Care Trust (BHSC), Royal  
23 Victoria Hospital (RVH), 274 Grosvenor Road, Belfast, BT12 6BA, Northern Ireland (UK)

24 <sup>6</sup> Veterinary Sciences Division, Agri-Food and Biosciences Institute (AFBI), Stormont, 12  
25 Stoney Road, Belfast, BT4 3SD, Northern Ireland (UK).

26 <sup>7</sup> Institute for Global Food Security (IGFS), Queen’s University Belfast, 19 Chlorine Gardens,  
27 Belfast, BT9 5DL, Northern Ireland (UK).

28

## 29 **Corresponding authors:**

30 Andrew J. Lee: [a.j.lee@qub.ac.uk](mailto:a.j.lee@qub.ac.uk) & Connor G. G. Bamford: [c.bamford@qub.ac.uk](mailto:c.bamford@qub.ac.uk)

31

32 **Keywords:** wastewater, epidemiology, surveillance, influenza, virus, avian, human,  
33 genomic, nanopore, sequencing

NOTE: This preprint reports new research that has not been certified by peer review and should not be used to guide clinical practice.

## Abstract

34  
35  
36  
37  
38  
39  
40  
41  
42  
43  
44  
45  
46  
47  
48  
49  
50  
51  
52  
53  
54  
55  
56  
57  
58  
59  
60  
61  
62

**Background:** Influenza A viruses (IAV) are significant pathogens of humans and other animals. Although endemic in humans and birds, novel IAV strains can emerge, jump species, and cause epidemics, like the latest variant of H5N1. Wastewater-based epidemiology (WBE) has very recently been shown to detect human IAV but whether it can detect avian-origin IAV, and if whole genome sequencing (WGS) can be used to discriminate circulating strains of IAV in wastewater remains unknown.

**Methods:** Using a pan-IAV RT-qPCR assay, six wastewater treatment works (WWTWs) across Northern Ireland (NI), were screened from August to December 2022. A WGS approach using Oxford Nanopore technology was employed to sequence positive samples. Phylogenetic analysis of sequences relative to currently circulating human and avian IAVs was performed.

**Findings:** We detected a dynamic IAV signal in wastewater from September 2022 onwards across NI. “Meta” whole genome sequences were generated displaying homology to both human and avian IAV strains. The relative proportion of human versus avian-origin IAV reads differed across time and sample site. A diversity in subtypes and lineages was detected (e.g. H1N1, H3N2, and several avian). Avian segment 8 related to those found in recent H5N1 clade 2.3.4.4b was identified.

**Interpretation:** WBE affords a means to monitor circulating human and avian IAV strains and provide crucial genetic information. As such WBE can provide rapid, cost-effective, year-round “one-health” IAV surveillance to help control epidemic and pandemic threats.

**Funding:** This study was funded by the Department of Health for Northern Ireland as part of the Northern Ireland Wastewater Surveillance Programme.

## 63 Highlights

64

- 65 • Dynamic IAV RT-qPCR signal in wastewater detected across NI.
- 66 • Nanopore-based WGS reveals presence of both human and avian IAVs in  
67 wastewater.
- 68 • Avian IAV sequence similarity to gull-associated H13/H16 and recent H5N1 isolates.
- 69 • Co-detection of distinct clades of human H1N1 and H3N2 subtypes.

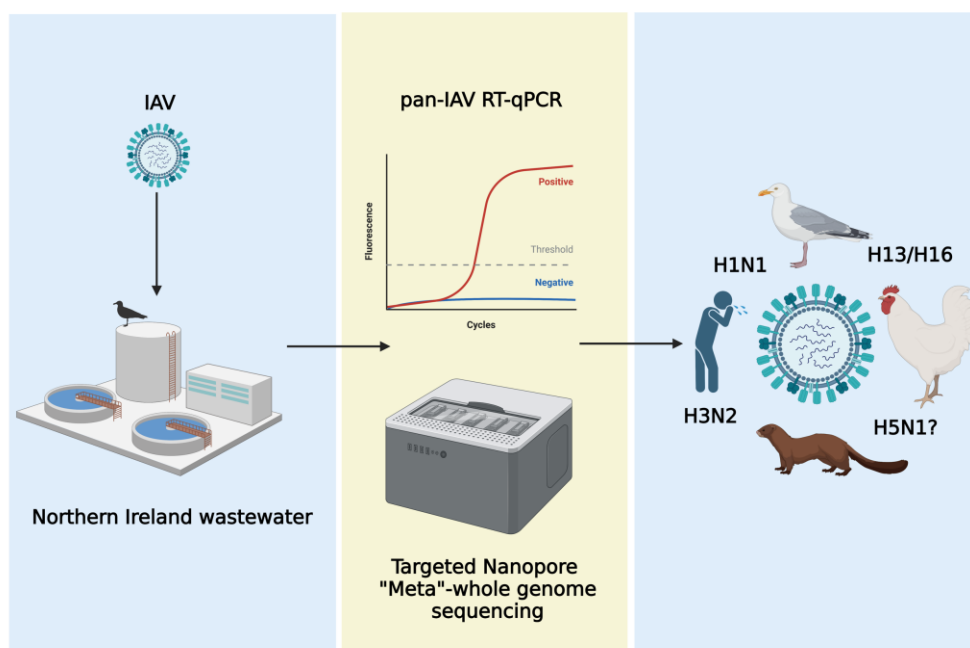
70

## 71 Author Summary

72 Influenza A virus (IAV) is a major pathogen of humans and other animals and causes regular  
73 epidemics and devastating pandemics. Recently, a novel variant of highly-pathogenic H5N1  
74 avian influenza has emerged spreading across the world killing millions of birds and infecting  
75 mammals, enhancing its pandemic potential. Strengthening global surveillance systems for  
76 human and animal IAV is thus a major priority. Wastewater-based epidemiology (WBE) has  
77 been applied to track SARS-CoV-2 and IAV in humans but whether this approach could  
78 work for avian IAV is not known. Here, we develop a “one-health” method to survey pan-IAV  
79 levels and genetically characterise the viruses. Through this we highlight co-detection of  
80 human and avian IAVs in wastewater, with homology to recent H5N1 isolates. Our work  
81 demonstrates the potential for WBE to help defend against not only human infections but  
82 emerging, zoonotic IAVs of pandemic potential.

83

## 84 Graphical Abstract



## Introduction

85

86

87 Influenza A virus (IAV) (Family *Orthomyxoviridae*; Genus *Influenzavirus*) is an enveloped  
88 virus with a genome comprising 8 segments (named 1-8) of single-stranded negative sense  
89 RNA (Krammer et al., 2018). The IAV genome encodes at least 10 proteins, including the  
90 hemagglutinin (HA) and neuraminidase (NA) glycoproteins, and the innate immune  
91 antagonist non-structural protein 1 (NS1). IAV is a major pathogen of humans, livestock,  
92 and wildlife, and is the causative agent of several pandemics over the last century following  
93 zoonosis from animal reservoirs like pigs and birds. Clinical burden in humans and animals  
94 is extensive (1,2,3) but can be managed through prophylactic vaccination focused towards  
95 circulating HA and NA sequences (4).

96

97 IAV has many subtypes and although some are endemic in humans (e.g., H1N1 and H3N2)  
98 and other mammals, wild birds belonging to the orders Anseriformes (e.g., ducks) and  
99 Charadriiformes (e.g., gulls [5]) are widely acknowledged as the major IAV genetic  
100 reservoirs. Most IAVs are considered low pathogenicity avian influenza viruses (LPAIVs)  
101 e.g., H13Nx and H16Nx that infect gulls (6,7,8). Others (e.g., H5 and H7) can be high  
102 pathogenicity avian influenza viruses (HPAIVs) due to the acquisition of a “multibasic  
103 cleavage sequence” in HA (9). A novel strain of H5Nx (clade 2.3.4.4b) HPAIV was first  
104 detected in 2016 in Eurasia (10). This variant spread globally killing over 50 million birds and  
105 infecting wild and farmed mammal species. Additional evidence suggesting mammal-to-  
106 mammal transmission (e.g., mink) increases the pandemic potential of such circulating  
107 HPAIVs, emphasising the need for heightened, active surveillance in both humans and  
108 animals (11,12).

109

110 Current human IAV monitoring usually entails clinical surveillance via primary care (sentinel  
111 GP services and in-hospital testing) with onward analysis of positive samples by PCR and  
112 sequencing. Avian IAV surveillance incorporates active (capture and swabbing of live birds)  
113 and passive (dead birds) monitoring. Environmental sampling (e.g., faeces or mud) has  
114 been explored but has not played a significant role in surveillance efforts globally (13).  
115 Complementing established clinical surveillance methods, WBE has recently proven an  
116 effective approach to track levels and identify variants of SARS-CoV-2 circulating in the  
117 human population (14,15,16). Likewise, this method has proven useful for the monitoring of  
118 enteric pathogens like adenoviruses (17), and other viruses such as respiratory syncytial  
119 virus (18,19). WBE studies have also demonstrated the detection of human IAV and

120 influenza B virus (IBV) in wastewater samples, using targeted PCR but with limited  
121 sequencing (20,21,22,23,24,25,26).

122

123 Whether WBE surveillance can be repurposed as a single sampling approach to monitor  
124 both human and animal viral reservoirs and thus help identify and characterise pathogens  
125 such as avian influenza with zoonotic potential, remains unknown. Here, we describe an  
126 integrated pan-IAV genomic WBE surveillance approach, using an RT-qPCR assay and  
127 nanopore WGS to rapidly sequence and subtype influenza positive samples detected and  
128 distinguish between human and avian sequences.

129

130

131  
132  
133  
134  
135  
136  
137  
138  
139  
140  
141  
142  
143  
144  
145  
146  
147  
148  
149  
150  
151  
152  
153  
154  
155  
156  
157  
158  
159  
160  
161  
162  
163  
164  
165

## Methods

### Sample Collection and Processing

Composite (24 hour) wastewater samples comprising primary untreated influent were collected using an Isco Glacier autosampler (Isco; Lincoln, USA) from 6 WWTW covering key population centres from each health trust of NI. Sampling was carried out by Northern Ireland Water Ltd and the Northern Ireland Environment Agency (NIEA). Once received, samples were stored at 4°C before pre-processing the same day. Sample processing, viral concentration, and extraction was carried out as previously described (17).

### Wastewater Screening for IAV - Matrix Protein (MP) segment RT-qPCR

Screening of wastewater for the presence of IAV employed the SVIP-MPv2 assay (27). Universal IAV detection was confirmed against avian (H6N1), human (H1N1 and H3N2) and swine (pH1N1 and H1N2) nucleic acid extracts prepared in-house from inactivated virus stocks supplied by the Agri-Food and Biosciences Institute (AFBI, Northern Ireland) and QUB. Raw wastewater samples spiked with cultured human H1N1 virus, inactivated using Triton X (1% w/v), were prepared. These were processed to determine the SVIP-MPv2 assays suitability for use against wastewater, to identify any sample matrix effects and to determine if processing methods were applicable for the recovery of IAV. Replicate PCR reactions (comprising 2x 6µl and 2x 3µl purified nucleic acid template volumes) per wastewater sample were performed on a LightCycler 480 II Real-Time PCR System (Roche Diagnostic Limited). RT-PCR was carried out in a reaction volume of 25µL using AgPath-ID™ One-Step Reagents (ThermoFisher Scientific) with primers and probe at a final concentration of 1.4µM and 0.4µM respectively, and supplemented with bovine serum albumin (0.2mg/ml, ThermoFisher Scientific) with the following thermo-profile: 50°C for 10mins, 95°C for 10mins followed by 45 cycles of 95°C for 10s and 60°C for 30s (Table S1 and S2). A standard curve and limit of detection (LOD) were calculated for the SVIP-MPv2 assay (Figure S1) using synthetic RNA respiratory virus controls H1N1 and H3N2 (103001, 103002, Twist Bioscience) serially diluted in 0.1X TE buffer (ThermoFisher Scientific) supplemented with a blocking nucleic acid (0.1µg/µl yeast tRNA, Sigma-Aldrich). IAV MP segment concentrations were normalised using wastewater flow rate and expressed as gene copies (g.c.) per 100,000 population equivalents (p.e.) per day as previously described (Reyne et al., 2022). Clinical data by epidemiological week covering molecular tests carried out for IAV was supplied by the Regional Virus Laboratory (RVL), Belfast Health and Social Care Trust (BHSCT), NI.

166 **Amplicon Generation for Sequencing - Multi-segment RT-PCR Approach (M-RTPCR)**  
167 A M-RTPCR approach to simultaneously amplify all eight segments of the IAV genome from  
168 IAV MP positive wastewater samples within a single PCR reaction was employed (28). Only  
169 those IAV positive WW samples with a Ct value of  $\leq 37$  were selected for amplicon  
170 generation. One step RT-PCR was carried out using SuperScript III One-Step RT-PCR  
171 reagents (ThermoFisher Scientific) with final concentrations of primers MBTuni-12 and  
172 MBTuni-13 (0.2 $\mu$ M each [Table S1]) in a total volume of 50 $\mu$ l (40 $\mu$ l reaction mix and 10 $\mu$ l of  
173 purified nucleic acid). Reactions were run in duplicate on a C1000 Touch thermal cycler  
174 (Biorad) using a 96 deep-well reaction module, following thermal cycling conditions as  
175 previously described (Table S2). Duplicate reaction mixtures were pooled, and amplified  
176 DNA purified using a 0.8X ratio of KAPA Pure Beads (Roche Diagnostic Limited).  
177 Quantification was carried out using a Qubit high-sensitivity double-stranded DNA kit (Qubit  
178 Flex, ThermoFisher Scientific), and amplicons analysed using D5000 ScreenTape assays  
179 (TapeStation 4200 System, Agilent Technologies) both according to the manufacturers'  
180 instructions (Figure S2). As an additional approach to further quantify generated amplicons  
181 prior to library preparation, 2  $\mu$ l of purified amplicon mix was re-tested using the SVIP-MPv2  
182 assay. A significant decrease in Ct value versus original screening Ct value was concomitant  
183 with the presence of increased amounts of matrix protein (segment 7) amplicons signifying  
184 successful genomic segment amplification (Table S3). To monitor for potential operator and  
185 environmental contamination as well as background nucleic acid present in reagents and  
186 consumables, negative process controls consisting of DEPC-treated nuclease free water  
187 (ThermoFisher Scientific) were included alongside and treated in the same manner.  
188

### 189 **Nanopore Library Preparation and Sequencing**

190 Samples were prepared for sequencing following the suggested protocol for ligation  
191 sequencing of gDNA with the SQK-LSK109 kit (Oxford Nanopore Technologies). To mitigate  
192 any problems of cross-barcode contamination samples were not multiplexed, instead a  
193 single sample per FLO-MIN106D R9 flow cell was sequenced on a GridION device (Oxford  
194 Nanopore Technologies) with sequencing proceeding for 24 hours. Negative process  
195 controls were also sequenced in the same way. Flow cells were only used once and not  
196 reused for subsequent IAV sequencing runs.

197

### 198 **Genomic Analysis**

199 Nanopore reads were base called using Guppy (version 6.4.2). Reads were taxonomically  
200 classified using Centrifuge (29). A total IAV read number of greater than 20 was arbitrarily



201 chosen as a cut-off for downstream analysis. Identified IAV reads were mapped using  
202 Minimap2 (30). For each sample, reference genomes encompassing potential originating  
203 viruses were utilised for mapping: human H1N1 (A/California/07/2009), H3N2  
204 (A/Barry/3792/2022; EPI\_ISL\_15391170), and avian H5N1  
205 (A/Mute\_Swan/Netherlands/2/2022; EPI\_ESL\_15364797) and H13N6 (A/black0headed  
206 gull/Netherlands/31/2014). Samtools was used for coverage calculations and BCFtools to  
207 generate consensus sequences (31). Alignment length and percentage coverage of raw  
208 reads was investigated using Basic Local Alignment Search Tool (BLAST+, version 2.13.0)  
209 against NCBI's available precompiled nucleotide database (32). Generated raw sequences  
210 are in the process of being submitted but are available on request.

211

## 212 **Phylogenetic Analyses**

213 Generated IAV consensus sequences were used for phylogenetic analysis. Consensus  
214 sequence incorporation differed depending on the analysis used with only homogenous  
215 consensus sequences used for interrogation of databases and phylogenetics of avian  
216 segments 5, 7 and 8, while all consensus sequences available were used for human  
217 segment 4 and 6 analysis. For human segment 4 and 6 analysis, Nextclade was used to  
218 remove low quality consensus sequences. Similarity to known sequences in the GISAID  
219 database was determined using their integrated BLAST protocol. All gull H13/16-like  
220 sequences since 2013, and H5N1 European sequences (2022) were used (downloaded  
221 January 2023). Select human H1N1 and H3N2 segment 4 and 6 sequences were used,  
222 including available recent sequences from Northern Ireland. Multiple sequence alignments  
223 were performed in MAFFT [<https://mafft.cbrc.jp/>], and maximum likelihood phylogenies  
224 inferred (1000 ultrafast bootstrap replicates) using IQ-TREE [<http://iqtree.cibiv.univie.ac.at/>]  
225 (33). The best substitution model was identified using IQ-TREE, ranked by BIC and  
226 implemented. Trees were visualised using FigTree v1.4.4  
227 [<http://tree.bio.ed.ac.uk/software/figtree/>]. Table S4 provides metadata on the GISAID  
228 genome sequences used in this study.

229

230



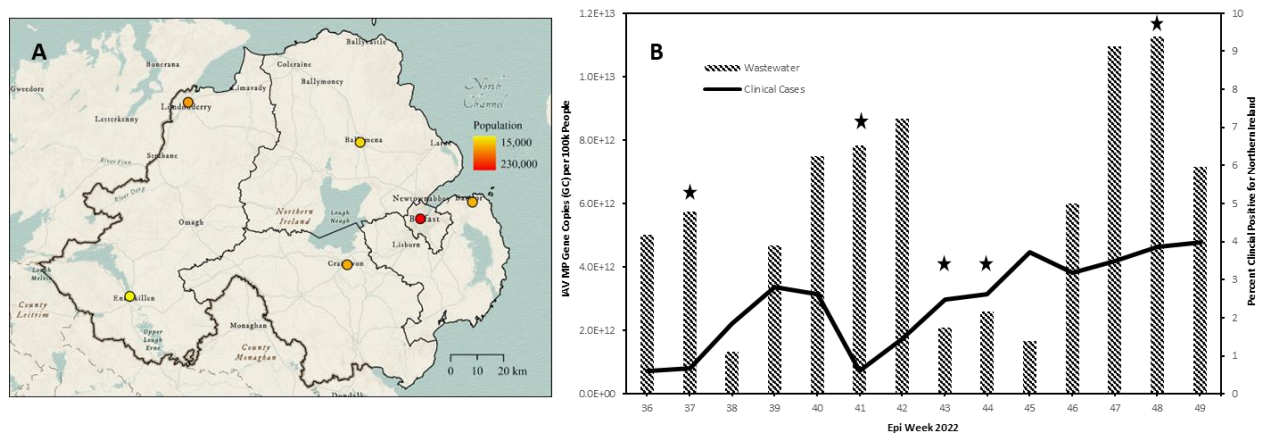
231

## Results

232

### 233 Pan-IAV wastewater screening by RT-qPCR

234 144 wastewater samples, from 6 WWTW across NI (**Figure 1 A**), were screened for IAV  
235 between 1<sup>st</sup> August 2022 and 5<sup>th</sup> December 2022 (epi weeks 31 - 49) using our pan-IAV  
236 assay. A consistent IAV signal above the LOD was first detected from the 5<sup>th</sup> of September  
237 2022 onwards (epi week 36), corresponding to an average weekly concentration of  $5.03 \times 10^{12}$  g.c.  
238  $10^{12}$  g.c. per 100k p.e. across the WWTW screened (**Figure 1 B**). IAV positivity and  
239 concentrations in wastewater varied across the sites sampled during the period investigated,  
240 with three peaks observed during weeks 37, 42 and 48, with an average of  $5.74 \times 10^{12}$ ,  $8.67$   
241  $\times 10^{12}$ , and  $1.13 \times 10^{13}$  g.c. per 100k p.e. respectively. Clinical data by epi week covering  
242 molecular tests carried out for IAV was supplied by the Regional Virus Laboratory, Royal  
243 Victoria Hospital. Clinical percentage positivity remained below 1% until week 35 (1.39%)  
244 and did not sustain an upwards trajectory until week 42 (1.44%), steadily increasing to  
245 3.99% during week 49 before rising markedly from week 50 onwards (6.42%) (**Figure 1 B**).  
246 The peak of the clinical influenza 2022/23 season was during week 52 (14.42% [data not  
247 shown]) outside of our study period.



248 **Fig 1. Dynamic IAV wastewater signal across NI.** Map showing geographical locations of WWTW  
249 across NI screened for IAV (A). West-to-East: Enniskillen, Derry/Londonderry, Craigavon, Ballymena,  
250 Belfast, and North Down. Normalised and averaged levels of IAV MP gene copies detected (g.c. per 100k  
251 p.e.) per epi week across the 6 WWTW sampled (B). Clinical data (black line) represents percentage IAV  
252 positive PCR and point of care tests carried out by the Regional Virus Laboratory for NI. ★ indicates epi  
253 weeks where IAV sequence was obtained.

254

### 255 Meta-whole genome sequencing of human and avian IAV from wastewater

256 The SVIP-MPv2 assay targets a highly conserved region of the IAV MP segment regardless  
257 of subtype and host. To resolve the genomic composition of detected IAV samples, a whole-  
258 genome amplification approach was employed. Overall, 12 of 36 IAV positive (<Ct 38)  
259 wastewater samples were successfully processed and sequenced (>20 IAV reads) following

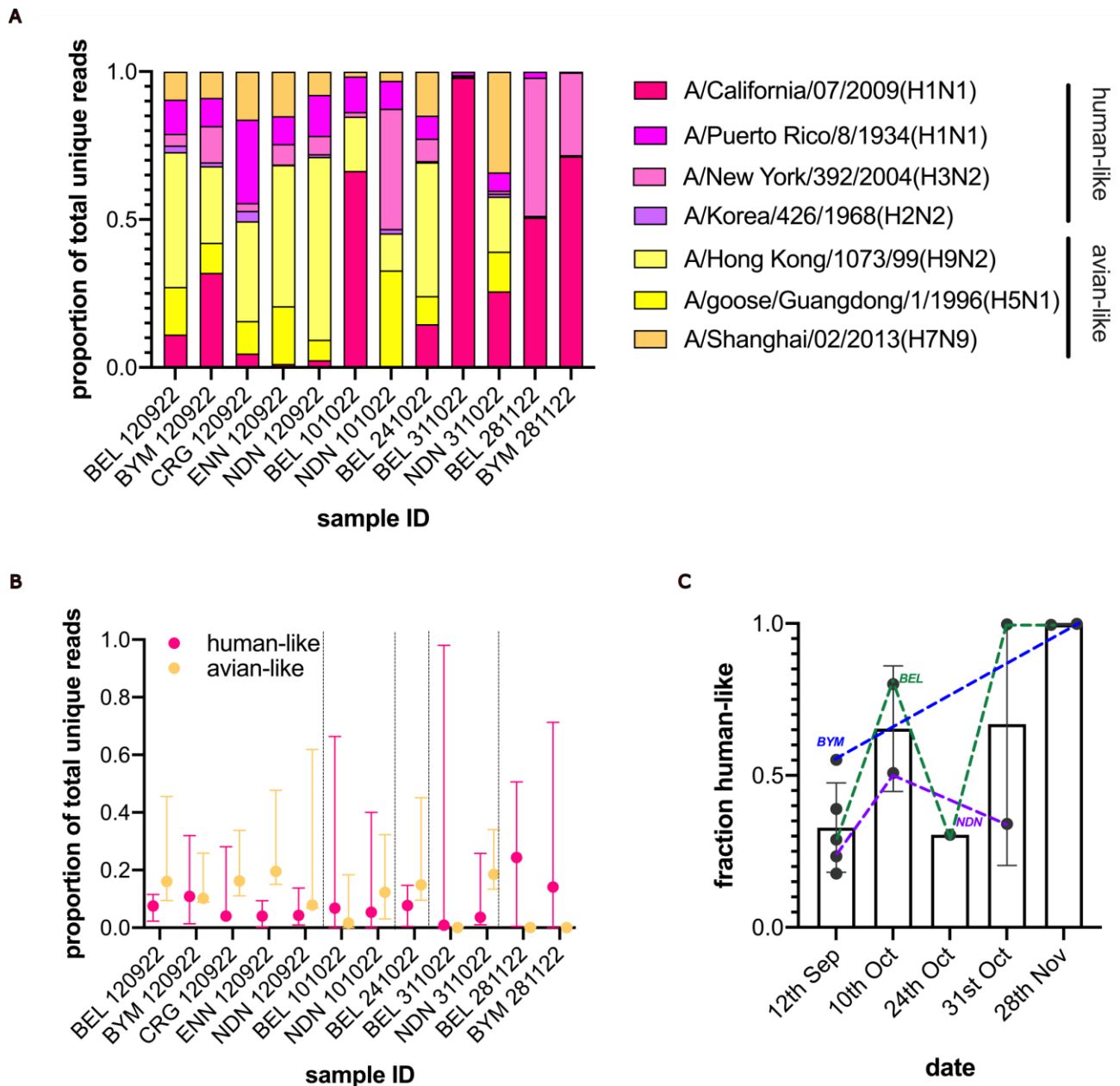
260 the full-segment amplicon generation method adopted (Zhou et al., 2009). IAV sequence  
 261 was generated from samples collected on 12/09/2022, 10/10/2022, 24/10/2022, 31/10/2022,  
 262 and 28/11/2022 (epi weeks 37-48 inclusive) covering a range of geographical locations (Fig  
 263 1A): West-to-East: Enniskillen (ENN), Craigavon (CRG), Ballymena (BYM), Belfast (BEL),  
 264 and North Down (NDN). No sequence data was obtained for Derry/Londonderry.  
 265

WwTW	Sample Date	Segment 1 PB2 (2.3kb)		Segment 2 PB1 (2.3kb)		Segment 3 PA (2.2kb)		Segment 4 HA (1.8kb)		Segment 5 NP (1.6kb)		Segment 6 NA (1.4kb)		Segment 7 MP (1.0kb)		Segment 8 NS (0.9kb)		Total Reads per Sample
		Reads	% Cover	Reads	% Cover	Reads	% Cover	Reads	% Cover	Reads	% Cover	Reads	% Cover	Reads	% Cover	Reads	% Cover	
Ballymena	12/09/2022	3	50.5	0	0	0	0	0	0	25	32.3	0	0	67	90.7	74	84.9	169
Belfast	12/09/2022	2	58	0	0	0	0	6	76.5	26	87	1	96.8	216	91.7	326	89.9	577
Craigavon	12/09/2022	2	91.6	35	25.7	0	0	112	33.3	13	88.2	4	76.4	277	92.7	167	91.1	610
Enniskillen	12/09/2022	0	0	0	0	0	0	0	0	18	78.2	31	95.7	347	96.1	228	93.8	624
North Down	12/09/2022	0	0	0	0	0	0	3	66	14	82.6	3	96	120	89.2	508	90.1	648
Belfast	10/10/2022	0	0	0	0	0	0	0	0	9	48.4	27	58.3	47	77.7	48	76.8	131
North Down	10/10/2022	0	0	0	0	0	0	0	0	5	86.7	0	0	60	88.7	0	0	65
Belfast	24/10/2022	0	0	0	0	0	0	0	0	0	0	12	87.1	507	96.7	676	92.1	1195
Belfast	31/10/2022	0	0	0	0	0	0	9	60.4	1	99.6	26	89.4	98	93.9	1306	90.4	1440
North Down	31/10/2022	0	0	0	0	0	0	0	0	0	0	0	0	96	93.4	0	0	96
Ballymena	28/11/2022	3	39.8	0	0	2	68.9	67	77.1	85	88.3	18	95.1	279	89.4	364	91.3	818
Belfast	28/11/2022	0	0	0	0	0	0	191	40.2	12	87.6	0	0	186	95.4	282	91.2	671
Per Segment																		
Total Reads & Average % Coverage		10	60	35	25.7	2	68.9	388	65.6	208	86.7	140	86.9	2,300	91.3	3,979	89.2	

266

267 **Table 1. Description of IAV WGS in wastewater.** Read number and average percentage coverage  
 268 per segment, per sample. Identity and alignment length of raw reads investigated using Basic Local  
 269 Alignment Search Tool against NCBI's available precompiled nucleotide database.  
 270

271 Identified IAV reads in these IAV RT-qPCR-positive samples ranged from 65 to 1,440, with  
 272 7,044 sequences detected overall. Reads were generally biased towards the smaller  
 273 segments (7 and 8) (**Table 1**). No single sample produced reads for every segment.  
 274 However, across the samples successfully sequenced, reads mapping to all 8 segments  
 275 were generated and referred to here as "meta"-WGS" to reflect sequencing all segments  
 276 and to distinguish from true WGS from clinical samples containing single strains. On  
 277 average, percentage coverage of segments varied considerably from 25.7% (PB1) up to  
 278 99.6% (NP). Sequences mapping to segments 4 and 6, encoding HA and NA, were  
 279 generated for 9 samples (75%). Average read number and coverage was 203/29.5% and  
 280 10.2/57.9% for HA and NA segments respectively.  
 281



282

283 **Fig 2. Taxonomic classification-first interrogation of IAV reads from wastewater.** Proportion unique  
 284 reads from samples (site: BEL = Belfast; BYM = Ballymena; CRG = Craigavon; NDN = North Down) were  
 285 assigned a similarity to 1 of 7 IAV strains (A/California/07/2009(H1N1); A/Puerto Rico/8/1934(H1N1);  
 286 A/New York/392/2004(H3N2); A/Korea/426/1968(H2N2); A/Hong Kong/1073/99(H9N2);  
 287 A/goose/Guangdong/1/1996(H5N1); A/Shanghai/02/2013(H7N9)) in the Centrifuge database. These  
 288 strains were grouped into human-like (H1N1, H3N2 and H2N2; purple shades) and avian-like (H9N2,  
 289 H5N1 and H7N9; yellow shades) (A). Data from A shown aggregated by human-like and avian-like for  
 290 each sample with median and range illustrated (B). Fractional proportion of aggregate human-like  
 291 sequences shown sample date only for all sites with links for those for which multirate data is available  
 292 (BEL in green, BYM in blue and NDN in purple) are shown (C). Graphs generated in Graphpad Prism  
 293 v9.0.

294

295 Initial read interrogation using a taxonomic classification first approach suggested the  
 296 presence of diverse IAV strains, possibly consisting of both human-like and avian-like  
 297 viruses (**Figure 2 A and B**). The relative abundance of these differed by sampling time and  
 298 site. At first heterogenous mixes predominated, but the relative abundance of human-like

299 IAV reads increased as the clinical influenza season commenced for Belfast and Ballymena  
 300 (**Figure 2 C**). However, North Down showed a more stable mix of human and avian-like  
 301 sequences. Furthermore, we generated consensus sequences by mapping, focussing our  
 302 downstream analysis on sequences where the consensus generated by each reference was  
 303 similar to each other. This resulted in 25 consensus sequences spanning all IAV segments  
 304 (described in **Table 2 and found in supplement**). Derived consensus sequences were  
 305 compared to known IAV sequences by BLAST, revealing diverse origins corroborating the  
 306 original analysis by Centrifuge, including human subtypes (H1N1 and H3N2) but also avian  
 307 subtypes, which are predominantly circulating in gull populations (H13N6), and even H5N1  
 308 clade 2.3.4.4b (Belfast 10/10/2022) from a Eurasian curlew (a member of the  
 309 Charadriiformes) (**Table 2**). Similar to the Centrifuge analysis, we detect here that the  
 310 proportion of avian-like sequences compared to human-like decreases at later sampling  
 311 dates.  
 312

WwTW	Sample Date	Segment	Mapping	Subtype	Host Species	GISAID ID	Name
Ballymena	12/09/2022	1	H1N1	H16N3	"gull"	EPI2181372	A/gull/Shandong/W1359/2021(A/H16N3) segment 1 (PB2)
Belfast	12/09/2022	1	H1N1	H13N8	black-headed gull	EPI1942887	A/Chroicocephalus_ridibundus/Belgium/13464/2020(A/H13N8) segment 1 (PB2)
Belfast	12/09/2022	5	H13N6	H13N2	Armenian gull	EPI617828	A/Armenian_gull/Republic_of_Georgia/2/2012(A/H13N2) segment 5 (NP)
Belfast	12/09/2022	6	H13N6	H13N6	common gull	EPI2195559	A/common_gull/Poland/MW241/2011(A/H13N6) segment 6 (NA)
Belfast	12/09/2022	8	H13N6	H13N6	black-headed gull	EPI889316	A/black-headed_gull/Netherlands/88/2012(A/H13N6) segment 8 (NS)
Craigavon	12/09/2022	1	H1N1	H16N3	"gull"	EPI2181372	A/gull/Shandong/W1359/2021(A/H16N3) segment 1 (PB2)
Craigavon	12/09/2022	2	H13N6	H13N8	common guillemot	EPI1884896	A/Common_guillemot/Sweden/SVA210729520317/FBO02610/I-2021(A/H13N8) segment 2 (PB1)
Craigavon	12/09/2022	6	H1N1	H1N1	human	EPI2124233	A/England/223980556/2022(A/H1N1_pdm09) segment 6 (NA)
Craigavon	12/09/2022	8	H13N6	H13N6	black-headed gull	EPI889316	A/black-headed_gull/Netherlands/88/2012(A/H13N6) segment 8 (NS)
Enniskillen	12/09/2022	5	H13N6	H13N8	common guillemot	EPI1884899	A/Common_guillemot/Sweden/SVA210729520317/FBO02610/I-2021(A/H13N8) segment 5 (NP)
Enniskillen	12/09/2022	6	H13N6	H13N6	common gull	EPI2195559	A/common_gull/Poland/MW241/2011(A/H13N6) segment 6 (NA)
North Down	12/09/2022	4	H13N6	H13N6	black-headed gull	EPI890024	A/black-headed_gull/Netherlands/5/2014(A/H13N6) segment 4 (HA)
North Down	12/09/2022	5	H13N6	H13N2	black-headed gull	EPI1014396	A/black-headed_gull/Netherlands/9/2014(A/H13N2) segment 5 (NP)
North Down	12/09/2022	8	H13N6	H13N6	black-headed gull	EPI889316	A/black-headed_gull/Netherlands/88/2012(A/H13N6) segment 8 (NS)
Belfast	10/10/2022	5	H1N1	H1N1	human	EPI2569903	A/France/ARA-HCLO23049801501/2023(A/H1N1_pdm09) segment 5 (NP)
Belfast	10/10/2022	6	H1N1	H1N1	human	EPI2550192	A/Poland/PL86/2022(A/H1N1_pdm09) segment 6 (NA)
Belfast	10/10/2022	7	H1N1	H1N1	human	EPI2295864	A/Catalonia/NSVH171694150/2022(A/H1N1_pdm09) segment 7 (MP)
Belfast	10/10/2022	8	H13N6	H13N8/H5N1	black-headed gull/Eurasian curlew	EPI1942894/EPI2540344	A/Chroicocephalus_ridibundus/Belgium/13464/2020(A/H13N8) segment 8 (NS)/A/Numenius_arquata/Belgium/01456_0003/2023(A/H5N1) segment 8 (NS)
North Down	10/10/2022	7	H13N6	H13N8	black-headed gull	EPI1942893	A/Chroicocephalus_ridibundus/Belgium/13464/2020(A/H13N8) segment 7 (MP)
Belfast	24/10/2022	6	H1N1	H1N1	human	EPI2550184	A/Ireland/67945/2022(A/H1N1_pdm09) segment 6 (NA)
Belfast	31/10/2022	6	H1N1	H1N1	human	EPI2141712	A/Czech_Republic/5176/2022(A/H1N1_pdm09) segment 6 (NA)
Belfast	31/10/2022	7	H1N1	H1N1	human	EPI2571961	A/Jamaica/7605/2023(A/H1N1_pdm09) segment 7 (MP)
Ballymena	28/11/2022	1	H3N2	H3N2	human	EPI2123118	A/Denmark/3021/2022(A/H3N2) segment 1 (PB2)
Ballymena	28/11/2022	3	H3N2	H3N2	human	EPI2193946	A/Barry/3792/2022(A/H3N2) segment 3 (PA)
Belfast	28/11/2022	5	H1N1	H1N1	human	EPI2571981	A/Costa_Rica/6859/2023(A/H1N1_pdm09) segment 5 (NP)

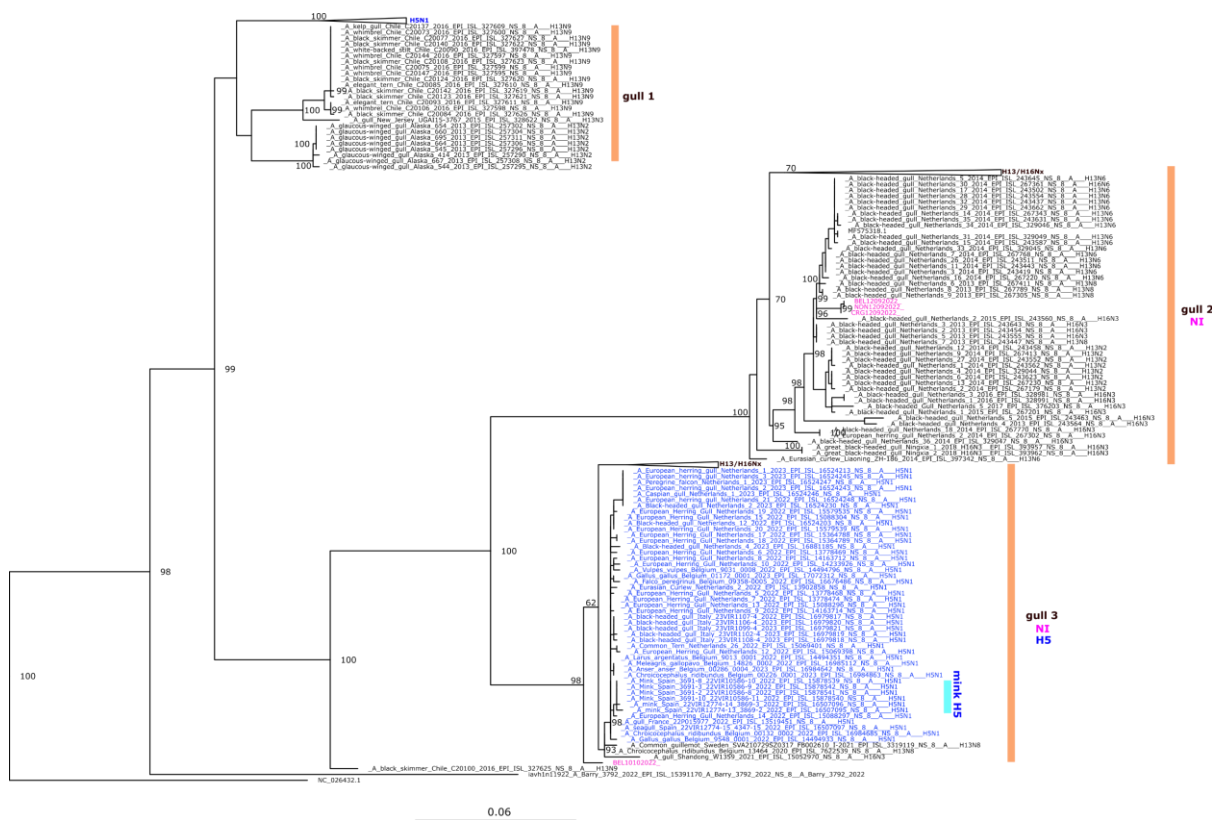
313  
 314 **Table 2: Similarity of wastewater IAV consensus sequences to known sequences.** Table describing  
 315 BLAST (GISAID) results for consensus sequences from samples sites and dates. Sequences spanned  
 316 all segments and interrogation of GISAID database allowed low resolution sub-typing by identifying  
 317 known subtype of the top-ranked similarity hit. For each top hit, the subtype, host species, GISAID ID and  
 318 name for each sequence is shown. For Belfast 10/10/2022 two hits are shown, including similarity to  
 319 H5N1.  
 320

### 321 **Detection of diverse lineages of gull-associated IAV in wastewater**

322 To explore the avian IAV sequences further, we determined the phylogenetic relatedness of  
 323 our derived consensus sequences relative to the two gull-associated sub-types (H13 and  
 324 H16 Nx) as well as recent (2022) H5N1 clade 2.3.4.4b viruses found across Europe.  
 325 Phylogenetic analysis of segment 8 (encoding the virulence factor NS1, and the essential  
 326 NEP) confirmed clear avian association but disclosed two distinct clades found in our  
 327 samples (**Figure 3**). One clade (gull 2; sequences found on 12-09-22) was closely related  
 328 to - but distinct from - H16Nx viruses identified in Europe in 2013/2015 (Netherlands). One



329 of these clades (gull 3; marked by Belfast 10-10-23) was more closely related to recent  
 330 European H5N1 viruses (clade 2.3.4.4b), which include viruses sequenced from birds and  
 331 mammals (mink). However, phylogenetically our H5N1-related sequence sat at a basal  
 332 position to the H5N1 sub-clade along with other gull-associated sequences (found in Europe  
 333 and China in 2020/21), suggesting that it is unlikely to be from an H5N1 viruses but from the  
 334 ancestor of the lineage that donated its segment 8 to H5N1 clade 2.3.4.4b. No other H5-like  
 335 sequences were detected. Interrogation of the three segment 5 sequences and the single  
 336 segment 7 sequence, identified similarity to sequences from Europe (2020/2021), China  
 337 (2021) and Alaska (2020) (Supplementary Figures 3 and 4).  
 338

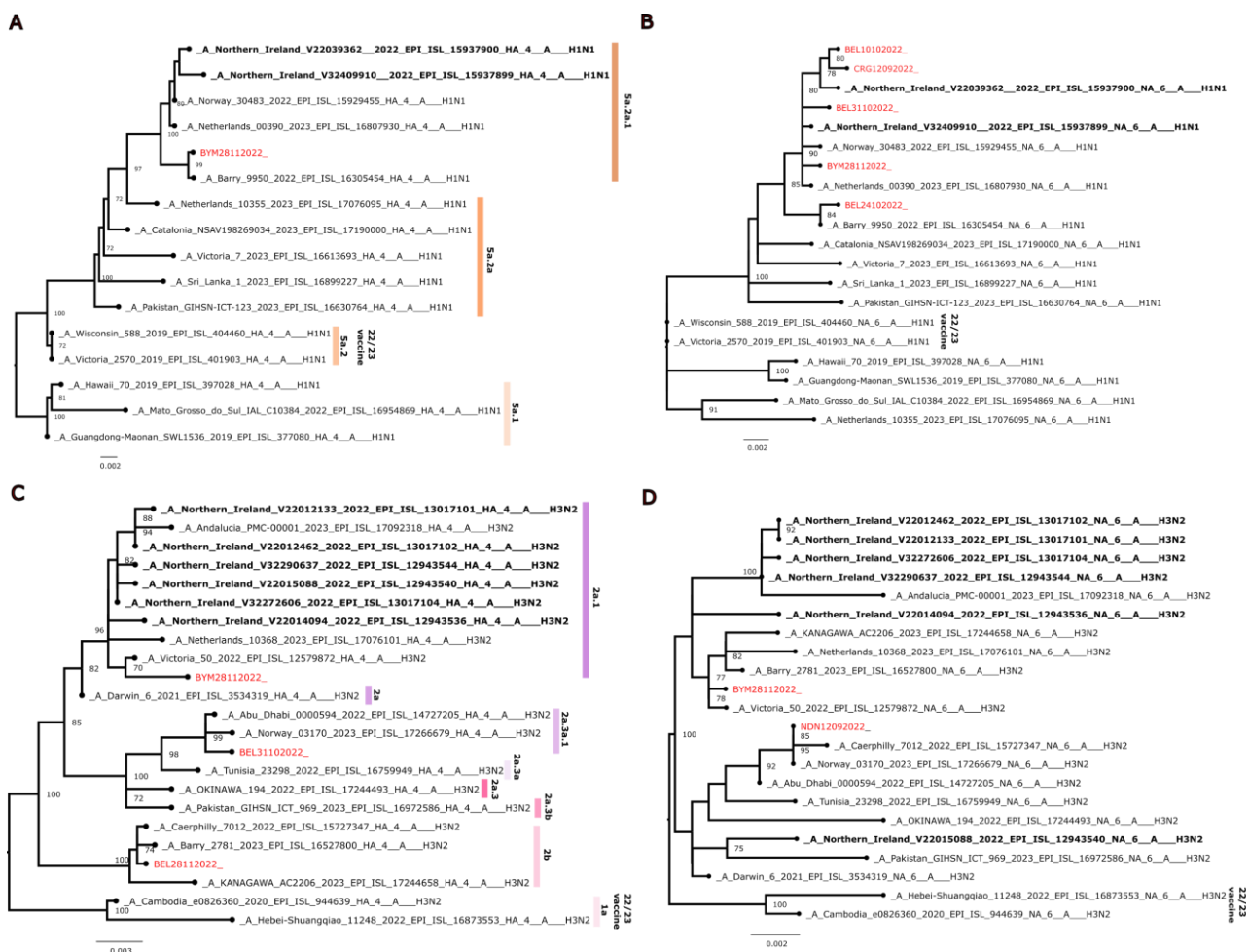


339  
 340  
 341 **Figure 3. Maximum-likelihood phylogeny of wastewater-derived avian-like segment 8 sequences.**  
 342 Phylogenetic tree of the 4 avian-like segment 8 sequences (in pink) alongside all GISAID gull H13/16-  
 343 like sequences (black), and 2022 H5N1 European sequences (in blue) (accessed January 2023). Three  
 344 clades are highlighted (gull 1 -3) with presence of NI (pink) and H5 (blue) annotated. Mink H5N1  
 345 sequences are highlighted in cyan. For illustrative purposes, several clades are shown collapsed in  
 346 cartoon form. Relevant bootstrap replicate values are shown on the tree.  
 347

348 **WBE reveals co-circulation of multiple lineages of human associated H1N1 and H3N2**  
 349 To determine whether our derived sequences might also provide information on the  
 350 evolution of the human epidemic, derived human epidemic, derived human segments 4 and 6 consensus sequences  
 351 were analysed further. To maximise the genomic information available, for this analysis, we  
 352 included all generated consensus sequences at our disposal, using Nextclade to identify

353 sequences of low quality that were subsequently removed from analysis. This resulted in 11  
 354 sequences from 7 samples (available in supplement). Phylogenetic analyses focused on our  
 355 segment 4 and 6 sequences compared to those from recently circulating IAVs from around  
 356 the world and 2022 Northern Ireland, demonstrated a diversity in WBE sequences, from at  
 357 least one H1N1 clade (6B.1A.5a.2a.1 [5a.2a.1]) and three H3N2 clades (all 'Bangladesh-  
 358 like' 3C.2a1b.2a.2a.1 [2a.1], 3C.2a1b.2a.2a.3a.1 [2a.3a.1], and 3C.2a1b.2a.2b [2b]) as  
 359 suggested by our initial analysis with Centrifuge (**Figure 4 A - D**). Our sequences were  
 360 similar to recently circulating strains in NI but phylogenetically distinct from those HA  
 361 sequences incorporated into the utilised vaccines (5a.2 for H1N1 and 3C.2a1b.2a.2 for  
 362 H3N2) for that season.

363



364

365 **Figure 4. Maximum-likelihood phylogeny of wastewater-derived human-like segment 4 (HA) and**  
 366 **6 (NA) sequences from H1N1 and H3N2.** Phylogenetic trees of the 11 human-like segment 4 and 6  
 367 sequences (in red) for H1N1 4 (A) and 6 (B) as well as H3N2 4 (C) and 6 (D) alongside select recent  
 368 worldwide sequences and all available relevant Northern Ireland (NI) clinical sequences (in bold black).  
 369 H1N1 NI clinical sequences were sampled during the 2022-2023 season, while the H3N2 NI clinical  
 370 sequences were sampled in Spring 2022 during the end of the 2021-2022 season. Established HA  
 371 sequence clades are shown alongside sequence groupings. Northern Hemisphere 2022/2023 winter  
 372 season vaccine strain sequences highlighted. Bootstrap replicate values >69 are only shown on the tree.

373

374

## Discussion

375

376 Here we show that WBE, a surveillance approach traditionally focused on monitoring human  
377 infections, can also be repurposed and through WGS be used to distinguish between  
378 circulating strains of the virus and characterise animal pathogens, in this instance avian IAV  
379 (Figure S5).

380

381 Like others, we detect a clear and dynamic IAV signal in wastewater samples, highlighting  
382 the utility of WBE for monitoring influenza (20,21,22,23,24,25,26). However, comparing our  
383 wastewater IAV viral load data from the 6 WWTW to the clinical % positivity rate across all  
384 of NI did not show a clear positive relationship. Like the rest of the UK (34), NI clinical  
385 positivity increased over time, while our IAV signal showed several clear peaks and troughs.  
386 WGS suggested that earlier in the season more avian IAV dominated before a later shift to  
387 human. Thus, considering our genomics findings, a lack of correlation may be expected  
388 given the overwhelming non-human avian IAV signal detected. This could potentially reflect  
389 dynamics of avian IAVs in wild avian reservoirs. Indeed, comparing peaks in early  
390 September and early October, distinct avian IAV strains were even identified. Alternatively,  
391 the lack of correlation could be explained by the lower % population coverage for the  
392 wastewater surveillance compared to clinical testing, which covers all NI.

393

394 Wastewater sequencing of IAV detected diverse avian IAV lineages, notably recent H13 and  
395 H16-like viruses, which are LPAIV subtypes infecting gulls and closely related species  
396 belonging to the order Charadriiformes, poultry and mammals (6,7,35,36,8). Remarkably,  
397 we identified one sequence (segment 8 BEL10102022) with close affinity to  
398 contemporaneous HPAI H5N1 viruses found across Europe, proven capable of spreading  
399 between mammals (12). Although recently in NI, gulls have been confirmed infected with  
400 H5N1 (37), it is unlikely that we detected the HPAIV H5N1 clade 2.3.4.4b as H5N1 homology  
401 was identified only for one segment (8; NS1/NEP), and phylogenetic analysis suggested  
402 that they fell outside of the recent H5N1 group. Indeed, we only found non-H5 avian H13  
403 segments with no H5 identified. Notably, recent European H5N1 viruses have reassorted  
404 with local gull-associated viruses, acquiring segments 3, 5 and 8 (12). Gulls have been  
405 shown to be important in spreading HPAIV H5 (38).

406

407 Previous WBE IAV studies, sampling at both the catchment and near source level, and using  
408 a variety of processing methods, have proven that molecular detection of IAV/IBV from both



409 solid and liquid WW fractions is possible, highlighting how effective this medium is for  
410 tracking influenza dynamics within human communities. However, these studies have  
411 usually adopted a human-centric screening and sequencing approach, possibly explaining  
412 why convincing evidence of avian IAV has not been reported thus far. It is also likely that  
413 timing and geography are factors impacting avian IAV detection. The stable mixture of  
414 human and avian IAV seen throughout the study period at the North Down WWTW may  
415 reflect to the coastal location of this site, which is close to important seabird colonies in  
416 Belfast Lough, the Copeland Islands and Strangford Lough (39). The other sampled WWTW  
417 sites (with the exception of Derry/Londonderry, from which no sequences were recovered)  
418 are located much further inland. Regarding the precise origin of our avian influenza  
419 sequences, WWTW in general are recognised as providing artificial habitats for birds year-  
420 round (40,41). However, without in-depth ecological studies at WWTW, other mechanisms  
421 must be considered - such as the role of mammal vectors (42) or that true human infection  
422 exists. However, we consider these scenarios less likely than direct avian deposition, as no  
423 human infections with H13 or H16 subtypes have been noted.

424

425 Our protocol generated sequence information from the early stages of the human 2022/23  
426 IAV epidemic in NI, in particular covering segments 4 (HA) and 6 (NA) that facilitate  
427 subtyping and antigenic comparison. Given the dearth of available clinical IAV sequences  
428 from NI, an accurate comparison between wastewater and the clinical would be challenging,  
429 although wastewater-derived sequences generally matched contemporary globally  
430 circulating viruses. Comparing our sequences with those of the chosen vaccine strains for  
431 2022/2023 showed phylogenetic distinctness, which may impact antigenicity although  
432 vaccine match was generally considered good for that year (43). This suggests that sensitive  
433 and effective real-time WBE IAV sequencing could be as a tool to inform in-season  
434 estimates of vaccine effectiveness and clinical burden. However, this would require further  
435 in-depth molecular and serological analysis of derived HA and NA sequences, and  
436 development of more specific RT-qPCR assays

437

438 We show that “meta” WGS of IAV from WW is possible, despite the unique challenges such  
439 complex sample matrices pose. The heterogenous mix of PCR inhibitors, fragmented state  
440 of shed virus and variations in viral titres present can negatively impact sequencing  
441 workflows. Capturing more virus material, reducing inhibitors, enhancing nucleic acid  
442 extraction/purification steps, using more robust enzyme systems, and updated sequencing  
443 reagent chemistries/technologies could improve sequencing outcomes. The choice of

444 bioinformatic workflow, and attendant reference databases, should also be carefully  
445 considered to enhance sensitivity and accuracy. Recently developed, influenza focussed  
446 bioinformatics tools, such as those provided by “EPI2ME Labs” (44) and “INSaFLU” (45),  
447 promise a streamlined approach to deal with primary data, but it remains to be seen how  
448 suitable these workflows are for analysing highly complex mixed environmental samples  
449 such as those from wastewater.

450

451 In conclusion, we demonstrate that human-centric WBE can be refocussed as a useful tool  
452 for combined avian and human IAV genomic surveillance. WBE may augment established  
453 veterinary and clinical testing structures, presenting opportunities to give advance warning  
454 on the incidence and spread of IAV and provide a cost-effective means to develop a global  
455 and sustained year-round “one health” sentinel service for IAV.

456

457

## References

458

459 (1) Krammer F, Smith GJD, Fouchier RAM, Peiris M, Kedzierska K, Doherty PC, Palese P,  
460 Shaw ML, Treanor J, Webster RG, García-Sastre A. Influenza. *Nat Rev Dis Primers*. 2018  
461 Jun 28;4(1):3. doi: 10.1038/s41572-018-0002-y. PMID: 29955068; PMCID: PMC7097467.

462

463 (2) Wang X, Li Y, O'Brien KL, Madhi SA, Widdowson MA, Byass P, Omer SB, Abbas Q, Ali  
464 A, Amu A, Azziz-Baumgartner E, Bassat Q, Abdullah Brooks W, Chaves SS, Chung A,  
465 Cohen C, Echavarria M, Fasce RA, Gentile A, Gordon A, Groome M, Heikkinen T, Hirve S,  
466 Jara JH, Katz MA, Khuri-Bulos N, Krishnan A, de Leon O, Lucero MG, McCracken JP,  
467 Mira-Iglesias A, Moïsi JC, Munywoki PK, Ourohiré M, Polack FP, Rahi M, Rasmussen ZA,  
468 Rath BA, Saha SK, Simões EA, Sotomayor V, Thamthitawat S, Treurnicht FK, Wamukoya  
469 M, Yoshida LM, Zar HJ, Campbell H, Nair H; Respiratory Virus Global Epidemiology  
470 Network. Global burden of respiratory infections associated with seasonal influenza in  
471 children under 5 years in 2018: a systematic review and modelling study. *Lancet Glob  
472 Health*. 2020 Apr;8(4):e497-e510. doi: 10.1016/S2214-109X(19)30545-5. Epub 2020 Feb  
473 20. PMID: 32087815; PMCID: PMC7083228.

474

475 (3) Uyeki TM, Hui DS, Zambon M, Wentworth DE, Monto AS. *Influenza*. *Lancet*. 2022 Aug  
476 27;400(10353):693-706. doi: 10.1016/S0140-6736(22)00982-5. PMID: 36030813; PMCID:  
477 PMC9411419.

478

- 479 (4) Wei CJ, Crank MC, Shiver J, Graham BS, Mascola JR, Nabel GJ. Next-generation  
480 influenza vaccines: opportunities and challenges. *Nat Rev Drug Discov.* 2020  
481 Apr;19(4):239-252. doi: 10.1038/s41573-019-0056-x. Epub 2020 Feb 14. Erratum in: *Nat*  
482 *Rev Drug Discov.* 2020 Jun;19(6):427. PMID: 32060419; PMCID: PMC7223957.  
483
- 484 (5) Yoon SW, Webby RJ, Webster RG. Evolution and ecology of influenza A viruses. *Curr*  
485 *Top Microbiol Immunol.* 2014;385:359-75. doi: 10.1007/82\_2014\_396. PMID: 24990620.  
486
- 487 (6) Hinshaw VS, Air GM, Gibbs AJ, Graves L, Prescott B, Karunakaran D. Antigenic and  
488 genetic characterization of a novel hemagglutinin subtype of influenza A viruses from gulls.  
489 *J Virol.* 1982 Jun;42(3):865-72. doi: 10.1128/JVI.42.3.865-872.1982. PMID: 7097861;  
490 PMCID: PMC256920.  
491
- 492 (7) Fouchier RA, Munster V, Wallensten A, Bestebroer TM, Herfst S, Smith D,  
493 Rimmelzwaan GF, Olsen B, Osterhaus AD. Characterization of a novel influenza A virus  
494 hemagglutinin subtype (H16) obtained from black-headed gulls. *J Virol.* 2005  
495 Mar;79(5):2814-22. doi: 10.1128/JVI.79.5.2814-2822.2005. PMID: 15709000; PMCID:  
496 PMC548452.  
497
- 498 (8) Verhagen JH, Poen M, Stallknecht DE, van der Vliet S, Lexmond P, Sreevatsan S,  
499 Poulson RL, Fouchier RAM, Lebarbenchon C. Phylogeography and Antigenic Diversity of  
500 Low-Pathogenic Avian Influenza H13 and H16 Viruses. *J Virol.* 2020 Jun  
501 16;94(13):e00537-20. doi: 10.1128/JVI.00537-20. PMID: 32321814; PMCID:  
502 PMC7307148.  
503
- 504 (9) Munster VJ, Schrauwen EJ, de Wit E, van den Brand JM, Bestebroer TM, Herfst S,  
505 Rimmelzwaan GF, Osterhaus AD, Fouchier RA. Insertion of a multibasic cleavage motif  
506 into the hemagglutinin of a low-pathogenic avian influenza H6N1 virus induces a highly  
507 pathogenic phenotype. *J Virol.* 2010 Aug;84(16):7953-60. doi: 10.1128/JVI.00449-10.  
508 Epub 2010 Jun 2. PMID: 20519405; PMCID: PMC2916526.  
509
- 510 (10) Lee DH, Sharshov K, Swayne DE, Kurskaya O, Sobolev I, Kabilov M, Alekseev A,  
511 Irza V, Shestopalov A. Novel Reassortant Clade 2.3.4.4 Avian Influenza A(H5N8) Virus in  
512 Wild Aquatic Birds, Russia, 2016. *Emerg Infect Dis.* 2017 Feb;23(2):359-360. doi:  
513 10.3201/eid2302.161252. Epub 2017 Feb 15. PMID: 27875109; PMCID: PMC5324796.

514

515 (11) WHO, 2022 [https://cdn.who.int/media/docs/default-source/influenza/avian-and-other-](https://cdn.who.int/media/docs/default-source/influenza/avian-and-other-zoonotic-influenza/h5-risk-assessment-dec-2022.pdf)  
516 [zoonotic-influenza/h5-risk-assessment-dec-2022.pdf](https://cdn.who.int/media/docs/default-source/influenza/avian-and-other-zoonotic-influenza/h5-risk-assessment-dec-2022.pdf)

517

518 (12) Agüero M, Monne I, Sánchez A, Zecchin B, Fusaro A, Ruano JM, del Valle Arrojo M,  
519 Fernández-Antonio R, Souto MA, Tordable P, Cañas J, Bonfante F, Giussani CTE, Orejas  
520 JJ. Highly pathogenic avian influenza A(H5N1) virus infection in farmed minks, Spain,  
521 October 2022. *Euro Surveill.* 2023;28(3):pii=2300001. [https://doi.org/10.2807/1560-](https://doi.org/10.2807/1560-7917.ES.2023.28.3.2300001)  
522 [7917.ES.2023.28.3.2300001](https://doi.org/10.2807/1560-7917.ES.2023.28.3.2300001)

523

524 (13) Hood G, Roche X, Brioudes A, von Dobschuetz S, Fasina FO, Kalpravidh W,  
525 Makonnen Y, Lubroth J, Sims L. A literature review of the use of environmental sampling  
526 in the surveillance of avian influenza viruses. *Transbound Emerg Dis.* 2021 Jan;68(1):110-  
527 126. doi: 10.1111/tbed.13633. Epub 2020 Jul 11. PMID: 32652790; PMCID:  
528 [PMC8048529](https://pubmed.ncbi.nlm.nih.gov/32652790/).

529

530 (14) Li, L., Uppal, T., Hartley, P.D., Gorzalski A., Pandori, M., Picker, A.M., Verma, S.C.,  
531 Pagilla, K. Detecting SARS-CoV-2 variants in wastewater and their correlation with  
532 circulating variants in the communities. *Sci Rep* 12, 16141 (2022).  
533 <https://doi.org/10.1038/s41598-022-20219-2>

534

535 (15) Bell SH, Allen DM, Reyne MI, Lock J, Fitzgerald A, Levickas A, Lee AJ, Bamford  
536 CGG, Gilpin DF, McGrath JW. Improved recovery of SARS-CoV-2 from wastewater  
537 through application of RNA and DNA stabilising agents. *Lett. Appl. Microbiol.* 2023,  
538 Volume 76, Issue 6, ovad047, <https://doi.org/10.1093/lambio/ovad047>

539

540 (16) Aparna Keshaviah, Megan B Diamond, Matthew J Wade, Samuel V Scarpino, Warish  
541 Ahmed, Fabian Amman, Olusola Aruna, Andrei Badilla-Aguilar, Itay Bar-Or, Andreas  
542 Bergthaler, Julie E Bines, Aaron W Bivins, Alexandria B Boehm, Jean-Martin Brault, Jean-  
543 Baptiste Burnet, Joanne R Chapman, Angela Chaudhuri, Ana Maria de Roda Husman,  
544 Robert Delatolla, John J Dennehy, Megan Beth Diamond, Celeste Donato, Erwin Duizer,  
545 Abiodun Egwuenu, Oran Erster, Despo Fatta-Kassinou, Aldo Gaggero, Deirdre F Gilpin,  
546 Brent J Gilpin, Tyson E Graber, Christopher A Green, Amanda Handley, Joanne Hewitt,  
547 Rochelle H Holm, Heribert Insam, Marc C Johnson, Rabia Johnson, Davey L Jones,  
548 Timothy R Julian, Asha Jyothi, Aparna Keshaviah, Tamar Kohn, Katrin G Kuhn,

- 549 Giuseppina La Rosa, Marie Lesenfants, Douglas G Manuel, Patrick M D'Aoust, Rudolf  
550 Markt, John W McGrath, Gertjan Medema, Christine L Moe, Indah Kartika Murni, Humood  
551 Naser, Colleen C Naughton, Leslie Ogorzaly, Vicka Oktaria, Christoph Ort, Popi Karaolia,  
552 Ekta H Patel, Steve Paterson, Mahbubur Rahman, Pablo Rivera-Navarro, Alex Robinson,  
553 Monica C Santa-Maria, Samuel V Scarpino, Heike Schmitt, Theodore Smith, Lauren B  
554 Stadler, Jorgen Stassijns, Alberta Stenico, Renee A Street, Elisabetta Suffredini, Zachary  
555 Susswein, Monica Trujillo, Matthew J Wade, Marlene K Wolfe, Habib Yakubu, Maria Ines  
556 Zanolli Sato. Wastewater monitoring can anchor global disease surveillance systems, *The*  
557 *Lancet Global Health*, Volume 11, Issue 6, 2023, Pages e976-e981, ISSN 2214-109X,  
558 [https://doi.org/10.1016/S2214-109X\(23\)00170-5](https://doi.org/10.1016/S2214-109X(23)00170-5).
- 559
- 560 (17) Reyne MI, Allen DM, Levickas A, Allingham P, Lock J, Fitzgerald A, McSparron C,  
561 Nejad BF, McKinley J, Lee A, Bell SH, Quick J, Houldcroft CJ, Bamford CGG, Gilpin DF,  
562 McGrath JW. Detection of human adenovirus F41 in wastewater and its relationship to  
563 clinical cases of acute hepatitis of unknown aetiology. *Sci Total Environ*. 2023 Jan  
564 20;857(Pt 2):159579. doi: 10.1016/j.scitotenv.2022.159579. Epub 2022 Oct 18. PMID:  
565 36270375.
- 566
- 567 (18) Allen DM, Reyne MI, Allingham P, Levickas A, Bell SH, Lock J, Coey JD, Carson S,  
568 Lee AJ, McSparron C, Nejad BF, McKenna JP, Shannon M, Li K, Curran T, Broadbent LJ,  
569 Downey DG, Power UF, Groves HE, McKinley JM, McGrath JW, Bamford CGG, Gilpin DF.  
570 Genomic Analysis and Surveillance of Respiratory Syncytial Virus (RSV) Using  
571 Wastewater-Based Epidemiology (WBE). medRxiv 2023.07.21.23293016; doi:  
572 <https://doi.org/10.1101/2023.07.21.23293016>
- 573
- 574 (19) Boehm AB, Hughes B, Duong D, Chan-Herur V, Buchman A, Wolfe MK, White BJ.  
575 Wastewater concentrations of human influenza, metapneumovirus, parainfluenza,  
576 respiratory syncytial virus, rhinovirus, and seasonal coronavirus nucleic-acids during the  
577 COVID-19 pandemic: a surveillance study. *Lancet Microbe*. 2023 May;4(5):e340-e348.  
578 doi: 10.1016/S2666-5247(22)00386-X. Epub 2023 Mar 22. PMID: 36965504; PMCID:  
579 PMC10032662.
- 580
- 581 (20) Mercier E, D'Aoust PM, Thakali O, Hegazy N, Jia JJ, Zhang Z, Eid W, Plaza-Diaz J,  
582 Kabir MP, Fang W, Cowan A, Stephenson SE, Pisharody L, MacKenzie AE, Graber TE,  
583 Wan S, Delatolla R. Municipal and neighbourhood level wastewater surveillance and

- 584 subtyping of an influenza virus outbreak. *Sci Rep.* 2022 Sep 22;12(1):15777. doi:  
585 10.1038/s41598-022-20076-z. PMID: 36138059; PMCID: PMC9493155.  
586
- 587 (21) Ando H, Ahmed W, Iwamoto R, Ando Y, Okabe S, Kitajima M. Impact of the COVID-  
588 19 pandemic on the prevalence of influenza A and respiratory syncytial viruses elucidated  
589 by wastewater-based epidemiology. *Sci Total Environ.* 2023 Jul 1;880:162694. doi:  
590 10.1016/j.scitotenv.2023.162694. Epub 2023 Mar 8. PMID: 36894088; PMCID:  
591 PMC9991320.  
592
- 593 (22) Dumke R, Geissler M, Skupin A, Helm B, Mayer R, Schubert S, Oertel R, Renner B,  
594 Dalpke AH. Simultaneous Detection of SARS-CoV-2 and Influenza Virus in Wastewater of  
595 Two Cities in Southeastern Germany, January to May 2022. *Int J Environ Res Public*  
596 *Health.* 2022 Oct 17;19(20):13374. doi: 10.3390/ijerph192013374. PMID: 36293955;  
597 PMCID: PMC9603229.  
598
- 599 (23) Markt R, Stillebacher F, Nägele F, Kammerer A, Peer N, Payr M, Scheffknecht C, Dria  
600 S, Draxl-Weiskopf S, Mayr M, Rauch W, Kreuzinger N, Rainer L, Bachner F, Zuba M,  
601 Ostermann H, Lackner N, Insam H, Wagner AO. Expanding the Pathogen Panel in  
602 Wastewater Epidemiology to Influenza and Norovirus. *Viruses.* 2023 Jan 17;15(2):263.  
603 doi: 10.3390/v15020263. PMID: 36851479; PMCID: PMC9966704.  
604
- 605 (24) Toribio-Avedillo D, Gómez-Gómez C, Sala-Comorera L, Rodríguez-Rubio L,  
606 Carcereny A, García-Pedemonte D, Pintó RM, Guix S, Galofré B, Bosch A, Merino S,  
607 Muniesa M. Monitoring influenza and respiratory syncytial virus in wastewater. Beyond  
608 COVID-19. *Sci Total Environ.* 2023 Sep 20;892:164495. doi:  
609 10.1016/j.scitotenv.2023.164495. Epub 2023 May 26. PMID: 37245831; PMCID:  
610 PMC10214770.  
611
- 612 (25) Vo V, Harrington A, Chang CL, Baker H, Moshi MA, Ghani N, Itorralba JY, Tillett RL,  
613 Dahlmann E, Basazinew N, Gu R, Familara TD, Boss S, Vanderford F, Ghani M, Tang AJ,  
614 Matthews A, Papp K, Khan E, Koutras C, Kan HY, Lockett C, Gerrity D, Oh EC.  
615 Identification and genome sequencing of an influenza H3N2 variant in wastewater from  
616 elementary schools during a surge of influenza A cases in Las Vegas, Nevada. *Sci Total*  
617 *Environ.* 2023 May 10;872:162058. doi: 10.1016/j.scitotenv.2023.162058. Epub 2023 Feb  
618 8. PMID: 36758698; PMCID: PMC9909754.



619

620 (26) Wolken M, Sun T, McCall C, Schneider R, Caton K, Hundley C, Hopkins L, Ensor K,  
621 Domakonda K, Kalvapalle P, Persse D, Williams S, Stadler LB. Wastewater surveillance of  
622 SARS-CoV-2 and influenza in preK-12 schools shows school, community, and citywide  
623 infections. *Water Res.* 2023 Mar 1;231:119648. doi: 10.1016/j.watres.2023.119648. Epub  
624 2023 Jan 20. PMID: 36702023; PMCID: PMC9858235.

625

626 (27) Nagy A, Vostinakova V, Pirchanova Z, Cernikova L, Dirbakova Z, Mojzis M, Jirincova  
627 H, Havlickova M, Dan A, Ursu K, Vilcek S, Hornickova J. Development and evaluation of a  
628 one-step real-time RT-PCR assay for universal detection of influenza A viruses from avian  
629 and mammal species. *Arch Virol.* 2010 May;155(5):665-73. doi: 10.1007/s00705-010-  
630 0636-x. Epub 2010 Mar 13. PMID: 20229116; PMCID: PMC7086820.

631

632 (28) Zhou B, Donnelly ME, Scholes DT, St George K, Hatta M, Kawaoka Y, Wentworth  
633 DE. Single-reaction genomic amplification accelerates sequencing and vaccine production  
634 for classical and Swine origin human influenza A viruses. *J Virol.* 2009 Oct;83(19):10309-  
635 13. doi: 10.1128/JVI.01109-09. Epub 2009 Jul 15. PMID: 19605485; PMCID:  
636 PMC2748056.

637

638 (29) Kim, D., Song, L., Breitwieser, F. P., & Salzberg, S. L. (2016). Centrifuge: Rapid and  
639 sensitive classification of metagenomic sequences. *Genome research*, 26(12), 1721-1729.  
640 <https://doi.org/10.1101/gr.210641.116>

641 Li, H. (2018). Minimap2: pairwise alignment for nucleotide sequences. *Bioinformatics*,  
642 34:3094-3100. doi:10.1093/bioinformatics/bty191

643

644 (30) Li, H. (2021). New strategies to improve minimap2 alignment accuracy.  
645 *Bioinformatics*, 37:4572-4574.

646

647 (31) Danecek P, Bonfield JK, Liddle J, Marshall J, Ohan V, Pollard MO, Whitwham A,  
648 Keane T, McCarthy SA, Davies RM, Li H. Twelve years of SAMtools and BCFtools.  
649 *Gigascience.* 2021 Feb 16;10(2):giab008. doi: 10.1093/gigascience/giab008. PMID:  
650 33590861; PMCID: PMC7931819.

651



- 652 (32) Camacho C, Coulouris G, Avagyan V, Ma N, Papadopoulos J, Bealer K, Madden TL.  
653 BLAST+: architecture and applications. BMC Bioinformatics. 2009 Dec 15;10:421. doi:  
654 10.1186/1471-2105-10-421. PMID: 20003500; PMCID: PMC2803857.  
655
- 656 (33) Trifinopoulos J, Nguyen LT, von Haeseler A, Minh BQ. W-IQ-TREE: a fast online  
657 phylogenetic tool for maximum likelihood analysis. Nucleic Acids Res. 2016 Jul  
658 8;44(W1):W232-5. doi: 10.1093/nar/gkw256. Epub 2016 Apr 15. PMID: 27084950;  
659 PMCID: PMC4987875.  
660
- 661 (34) UKSHA, 2023 [https://www.gov.uk/government/statistics/national-flu-and-covid-19-](https://www.gov.uk/government/statistics/national-flu-and-covid-19-surveillance-reports-2022-to-2023-season)  
662 [surveillance-reports-2022-to-2023-season](https://www.gov.uk/government/statistics/national-flu-and-covid-19-surveillance-reports-2022-to-2023-season)  
663
- 664 (35) Groth M, Lange J, Kanrai P, Pleschka S, Scholtissek C, Krumbholz A, Platzer M,  
665 Sauerbrei A, Zell R. The genome of an influenza virus from a pilot whale: Relation to  
666 influenza viruses of gulls and marine mammals. Infection, Genetics and Evolution, Volume  
667 24, 2014, Pages 183-186, ISSN 1567-1348, <https://doi.org/10.1016/j.meegid.2014.03.026>.  
668
- 669 (36) Yu Z, Cheng K, Gao Y. Poultry Infection with Influenza Viruses of Wild Bird Origin,  
670 China, 2016. Emerg Infect Dis. 2018 Jul;24(7):1375-1377. doi: 10.3201/eid2407.171220.  
671 PMID: 29912711; PMCID: PMC6038736.  
672
- 673 (37) DAERA NI, 2023 <https://www.daera-ni.gov.uk/articles/latest-situation>  
674
- 675 (38) Hill NJ, Bishop MA, Trovão NS, Ineson KM, Schaefer AL, et al. (2022) Ecological  
676 divergence of wild birds drives avian influenza spillover and global spread. PLOS  
677 Pathogens 18(5): e1010062 <https://doi.org/10.1371/journal.ppat.1010062>  
678
- 679 (39) Booth Jones, K. The Northern Ireland Seabird Report 2022. British Trust for  
680 Ornithology, ISBN: 978-1-912642-36-6.  
681
- 682 (40) Gough, S., Gillings, S. & Vickery, J.A. 2003. The value and management of  
683 wastewater treatment works for breeding and wintering birds in lowland eastern England.  
684 BTO Research Report no. 333.  
685

- 686 (41) Murray, C.G. and Hamilton, A.J. (2010), REVIEW: Perspectives on wastewater  
687 treatment wetlands and waterbird conservation. *Journal of Applied Ecology*, 47: 976-985.  
688 <https://doi.org/10.1111/j.1365-2664.2010.01853.x>  
689
- 690 (42) Velkers FC, Blokhuis SJ, Veldhuis Kroeze EJB, Burt SA. The role of rodents in avian  
691 influenza outbreaks in poultry farms: a review. *Vet Q.* 2017 Dec;37(1):182-194. doi:  
692 10.1080/01652176.2017.1325537. PMID: 28460593.  
693
- 694 (43) ECDC, 2023 <https://www.cdc.gov/mmwr/volumes/72/wr/mm7208a1.htm>  
695
- 696 (44) EPI2ME Labs, <https://labs.epi2me.io/>  
697
- 698 (45) Borges, V., Pinheiro, M., Pechirra, P. et al. INSaFLU: an automated open web-based  
699 bioinformatics suite “from-reads” for influenza whole-genome-sequencing-based  
700 surveillance. *Genome Med* 10, 46 (2018). <https://doi.org/10.1186/s13073-018-0555-0>